Anomalous integer quantum Hall effect in AA-stacked bilayer graphene

Ya-Fen Hsu[1] and Guang-Yu Guo[2,1,*]

[1]*Department of Physics and Center for Theoretical Sciences, National Taiwan University, Taipei 106, Taiwan*

[2]*Graduate Institute of Applied Physics, National Chengchi University, Taipei 116, Taiwan*

(Dated: August 5, 2010)

Recent experiments indicate that AA-stacked bilayer graphenes (BLG) could exist. Since the energy bands of the AA-stacked BLG are different from both the monolayer and AB-stacked bilayer graphenes, different integer quantum Hall effect in the AA-stacked graphene is expected. We have therefore calculated the quantized Hall conductivity σ_{xy} and also longitudinal conductivity σ_{xx} of the AA-stacked BLG within the linear response Kubo formalism. Interestingly, we find that the AA-stacked BLG could exhibit both conventional insulating behavior (the $\bar{\nu}=0$ plateau) and chirality for $|\bar{\mu}|<t$, where $\bar{\nu}$ is the filling factor ($\bar{\nu}=\sigma_{xy}h/e^2$), $\bar{\mu}$ is the chemical potential, and t is the interlayer hopping energy, in striking contrast to the monlayer graphene (MLG) and AB-stacked BLG. We also find that for $|\bar{\mu}|\neq[(\sqrt{n_2}+\sqrt{n_1})/(\sqrt{n_2}-\sqrt{n_1})]t$, where $n_1=1,2,3,\cdots$, $n_2=2,3,4,\cdots$ and $n_2>n_1$, the Hall conductivity is quantized as $\sigma_{xy}=\pm\frac{4e^2}{h}n$, $n=0,1,2,\cdots$, if $|\bar{\mu}|<t$ and $\sigma_{xy}=\pm\frac{4e^2}{h}n$, $n=1,2,3,\cdots$, if $|\bar{\mu}|>t$. However, if $|\bar{\mu}|=[(\sqrt{n_1}+\sqrt{n_2})/(\sqrt{n_2}-\sqrt{n_1})]t$, the $\bar{\nu}=\pm4(n_1+n_2)n$ plateaus are absent, where $n=1,2,3,\cdots$, in comparison with the AB-stacked BLG within the two-band approximation. We show that in the low-disorder and high-magnetic-field regime, $\sigma_{xx}\to0$ as long as the Fermi level is not close to a Dirac point, where Γ denotes the Landau level broadening induced by disorder. Furthermore, when σ_{xy} is plotted as a function of $\bar{\mu}$, a $\bar{\nu}=0$ plateau appears across $\bar{\mu}=0$ and it would disappear if the magnetic field $B=\pi t^2/Nehv_F^2$, $N=1,2,3,\cdots$. Finally, the disappearance of the zero-Hall conductivity plateau is always accompanied by the occurence of a $8e^2/h$-step at $\bar{\mu}=t$.

PACS numbers: 73.43.Cd,71.70.Di,72.80.Vp,73.22.Pr

I. INTRODUCTION

Graphene exhibits many peculiar properties[1] and has greatly intrigued physicists in recent years. Charge carriers in the monolayer graphene (MLG) possess a linear energy dispersion (see Fig. 1a)[2] and are of chiral nature[3] near each Dirac point. The quasiparticles in the AB-stacked bilayer graphene (BLG) are also chiral. However, unlike MLG, the energy spectra of the AB-stacked BLG are parabolic (Fig. 1b). One of the interesting properties of graphene is quantum Hall effect (QHE). Indeed, both theoretical[4] and experimental works[5–7] show that integer quantum Hall effect (IQHE) in MLG is unconventional. The Hall conductivity in MLG is quantized as $\sigma_{xy}=\pm\frac{4e^2}{h}(n+\frac{1}{2})$, where $n=0,1,2,\cdots$. The factor 4 comes from the fourfold (spin and valley) degeneracy. Furthermore, beacuse the states are shared by electron and hole at the zeroth Landau level (LL), the shift of 1/2 occurs. In contrast, in the AB-stacked BLG, within the two-band parabolic approximation, the Hall conductivity was shown to be $\sigma_{xy}=\pm\frac{4e^2}{h}n$, where $n=1,2,3,\cdots$[8]. The zeroth and first Landau levels are degenerate and hence the first quantum Hall plateau appears at $4e^2/h$ instead of $2e^2/h$. This phenomenon has been observed experimentally[9]. QHE of the AB-stacked BLG was also studied based on a four-band Hamiltoian in Ref. [10].

Although AB stacking is predicted to be energetically favored over AA stacking in *ab initio* density functional theory (DFT) calculations, the energy difference of about 0.02 eV/cell is small[11, 12]. Moreover, Lauffer *et al.* found that scanning tunneling microscopy (STM) images of BLG resemble that of MLG, and hence they regarded it as a consequence of the BLG confiqurration being close to AA stacking[13]. Moreover, Liu *et al.* reported that in their high-resolution transmission electron microscope (HR-TEM) experiments a high proportion of thermally treated samples are AA-stacked BLG[14]. These findings indicate the possibilty of fabrication of the AA-stacked BLG. Since the energy bands of the AA-stacked BLG (see Fig. 1c) are different from both the AB-stacked BLG and monolayer graphene, the quantum Hall effect in the AA-stacked is expected to be quite different from that in the latter two systems.

We have therefore carried out a theoretical study of IQHE as well as the longitudinal conductivity σ_{xx} in the AA-stacked bilayer graphene using the Kubo formalism. In this paper, we present a general analytical form of the Hall conductivity $[\sigma_{xy}(\bar{\mu},B)]$ as a function of both chemical potential ($\bar{\mu}$) and magnetic field (B) of the AA-stacked BLG. Our presentation will be divided into two parts: i) the variation of the σ_{xy} vs. $1/B$ curve with some fixed $\bar{\mu}$'s and ii) the effect of the magnetic field on the σ_{xy} vs. $\bar{\mu}$ curve. Our main findings are as follows. Firstly, for $|\bar{\mu}|\neq[(\sqrt{n_2}+\sqrt{n_1})/(\sqrt{n_2}-\sqrt{n_1})]t$, where t is the interlayer hopping energy, n_1 and n_2 are any integers larger than 1 and 2, respectively, and $n_1<n_2$, the Hall

*Electronic address: gyguo@phys.ntu.edu.tw

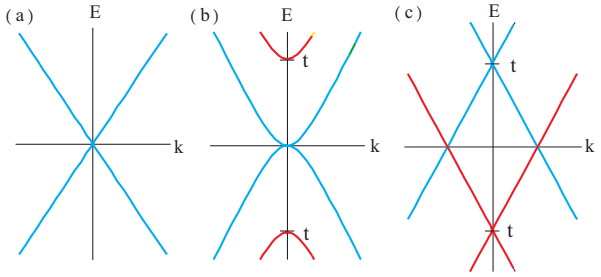

FIG. 1: (color online) The energy bands of (a) monolayer graphene, (b) AB-stacked bilayer graphene, and (c)AA-stacked bilayer graphene.

conductivity is quantized as

$$\sigma_{xy} = \pm\frac{4e^2}{h}n,\ n = 0, 1, 2, \cdots,\ \text{if } |\bar{\mu}| < t$$
$$\sigma_{xy} = \pm\frac{4e^2}{h}n,\ n = 1, 2, 3, \cdots,\ \text{if } |\bar{\mu}| > t. \quad (1)$$

However, if $|\bar{\mu}| = [(\sqrt{n_2}+\sqrt{n_1})/(\sqrt{n_2}-\sqrt{n_1})]t$, the Hall conductivity is given by

$$\sigma_{xy} = \pm\frac{4e^2}{h}n, \text{ excluding } \pm\frac{4e^2}{h}(n_1+n_2)n,\ n = 1, 2, 3, \cdots. \quad (2)$$

Secondly, in the low-disorder and high-magnetic-field regime [$\Gamma \to 0$ and $\hbar^4\omega_c^4 \gg (\bar{\mu}+\nu t)^4$], $\sigma_{xx} \approx (8e^2/\pi h)[(\bar{\mu}^2+t^2)\Gamma^2/(\bar{\mu}^2-t^2)^2 + 2\Gamma^2/\hbar^2\omega_c^2 + 5(\bar{\mu}^2+t^2)\Gamma^2/\hbar^4\omega_c^4)] \to 0$ if the Fermi level is not close to a Dirac point, where $\hbar\omega_c$ is the cyclotron energy. That is to say, if the magnetic field is high enough, the applied electric field cannot drive any current for $|\bar{\mu}| < t$, while the current is perpendicular to external electric field for $|\bar{\mu}| > t$. Thirdly, we find that the $\sigma_{xy} = 0$ (the filling factor $\bar{\nu} = 0$) plateau across $\bar{\mu} = 0$ would disappear when $B = \pi t^2/Nehv_F^2$, $N = 1, 2, 3, \cdots$, and that a $8e^2/h$-step at $\bar{\mu} = t$ occurs while a zero-Hall conductivity plateau disappears. Interestingly, unlike the monolayer and AB-stacked bilayer graphenes, the AA-stacked bilayer graphene could display a unusual $\bar{\nu} = 0$ plateau even though it contains chiral quasiparticles. We argue that the occurrence of the $\bar{\nu} = 0$ plateau is due to the shift of level anomalies by the interlayer hopping energy t.

II. THEORETICAL MODEL AND ANALYTICAL CALCULATION

A. Model Hamiltonian and Landau levels

We first derive an effective four-band Hamiltonian near each Dirac point for the AA-stacked bilayer graphene in tight-binding aprroximation via $\mathbf{k}\cdot\mathbf{p}$ expansion[1]. We then diagonalize this Hamiltonian to obtain the energy bands of the AA-stacked BLG. In Fig. 1, we display the energy bands of the MLG, AB-stacked, and AA-stacked BLG together. We find that the energy bands of the AA-stacked BLG are just two copies of the MLG band structure shifted up and down by t, respectively. Hence, $E = \pm t$ are the Dirac points for the AA-stacked BLG. When a magnetic field is applied, we should replace the momentum operator $\mathbf{p}$ with $\mathbf{p} + e\mathbf{A}/c$, where the external magnetic field $\mathbf{B} = \nabla\times\mathbf{A}$ and -e is the charge of an electron. The magnetic field is applied along the positive z-axis (i.e. out of plane) and hence the vector potential can be written as $\mathbf{A} = (-By, 0, 0)$ in the Landau gauge. Therefore, the effective four-band Hamiltonian in the presence of the magnetic field is given by

$$H_\pm = \begin{pmatrix} v_F(\sigma_x\pi_x \pm \sigma_y\pi_y) & -tI \\ -tI & v_F(\sigma_x\pi_x \pm \sigma_y\pi_y) \end{pmatrix}$$
$$: \begin{cases} \pi_x = -i\hbar\partial_x - eBy/c, \\ \pi_y = -i\hbar\partial_y. \end{cases} \quad (3)$$

Here $\pm$ label the two valleys of the band structure at K and K', respectively. v_F denotes the Fermi velocity. In the Laudau gauge, we can substitute the eigenfunction $\psi = e^{ikx}\phi(y)$ of the Hamiltonian into the schrödinger equation $H\psi = E\psi$. Here $\phi(y)$ can be written as $(\phi_1(y), \phi_2(y))^T$, where ϕ_1 and ϕ_2 are two-component column vectors. Then, we make the transformations: $\sigma^\pm = \sigma_x \pm i\sigma_y$, $\xi = y/\ell_B - \ell_B k$ and $O^\mp = (\xi \pm \partial_\xi)/\sqrt{2}$, where the magnetic length $\ell_B = \sqrt{\hbar c/|eB|}$. Finally, for the K valley, the schrödinger equation reads

$$\begin{pmatrix} \frac{-\hbar v_F}{\sqrt{2}\ell_B}(O^-\sigma^+ + O^+\sigma^-) & -tI \\ -tI & \frac{-\hbar v_F}{\sqrt{2}\ell_B}(O^-\sigma^+ + O^+\sigma^-) \end{pmatrix} \begin{pmatrix} \phi_1 \\ \phi_2 \end{pmatrix}$$
$$= E\begin{pmatrix} \phi_1 \\ \phi_2 \end{pmatrix}. \quad (4)$$

Since $O^\mp$ satisfy the commutation relation: $[O^-, O^+]$= 1, $O^\mp$ are the annihilation and creation operators of one-dimensional (1-D) simple harmonic oscillator (SHO), respectively. Similarly, $\sigma^\pm$ are the raising and lowering operators of pesudospin angular momentum. Obviously, the eigenstates of $O^-\sigma^+ + O^+\sigma^-$ are $(|N-1\rangle, \pm|N\rangle)^T$ if $N \geq 1$ and $(0, |0\rangle)^T$ if $N = 0$, where $|N\rangle$ are the eigenstates of the 1-D SHO. All non-zero vectors are eigenvectors of $-tI$. Therefore, we can infer that the eigenvalues of Eq. (4) are

$$E_N^{\mu\nu} = -\mu\sqrt{N}\hbar\omega_c - \nu t \quad (5)$$

with $\omega_c = \sqrt{2}v_F/\ell_B$ and the eigenstates of Eq. (4) are

$$\begin{cases} |0, +, \nu\rangle = \frac{1}{\sqrt{2}}\begin{pmatrix} 0 \\ |0\rangle \\ 0 \\ \nu|0\rangle \end{pmatrix}, & \text{if } N = 0, \\ |N, \mu, \nu\rangle = \frac{1}{2}\begin{pmatrix} |N-1\rangle \\ \mu|N\rangle \\ \nu|N-1\rangle \\ \mu\nu|N\rangle \end{pmatrix}, & \text{if } N \geq 1, \end{cases} \quad (6)$$

Here the indice $\mu = \pm$ and $\nu = \pm$. Clearly, the LLs of the AA-stacked BLG are just two copies of the LLs of the MLG shifted up and down by t, respectively.

B. Linear response calculation

The conductivity can be calculated using the Kubo formula within the linear response theory[15]. The Kubo formula for the DC-conductivity is given by

$$\sigma_{ij} = \lim_{\Omega\to 0} \frac{\mathrm{Im}\Pi^R_{ij}(\Omega + i0)}{\hbar\Omega}. \tag{7}$$

Here the retarded current-current correlation Π^R_{ij} in the Matsubara form reads[10]

$$\Pi^R_{ij}(i\nu_m) = -\frac{4e^2}{2\pi\ell_B^2\beta\hbar}\times \tag{8}$$
$$\sum_{n=-\infty}^{\infty}\sum_{k,\ell=0}^{\infty}\sum_{\substack{\mu,\rho\\=\pm}}\sum_{\substack{\nu,\sigma\\=\pm}} \frac{\langle k,\mu,\nu|v_i|\ell,\rho,\sigma\rangle\langle\ell,\rho,\sigma|v_j|k,\mu,\nu\rangle}{(i\tilde{\omega}_n - \tilde{E}^{\mu\nu}_k)(i\tilde{\omega}_n + i\nu_m - \tilde{E}^{\rho\sigma}_\ell)},$$

where the factor 4 is due to the fourfold (spin and valley) degeneracy, the velocity operator $v_i = [x_i\ H_+]/i\hbar$, and $\tilde{E}^{\mu\nu}_k = E^{\mu\nu}_k/\hbar$. ω_n and ν_m are Matsubara frequencies of fermion and boson, respectively. When the chemical potential and disorder scattering are considered, Matsubara frequency of fermion has to be corrected as $i\tilde{\omega}_n = i\omega_n + \bar{\mu}/\hbar + i\mathrm{sgn}(\omega_n)\Gamma/\hbar$. Γ is the Landau level broadening due to the presence of disorder. Substituting the eigenstates of H_+ into Eq. (8), we obtain

$$\Pi^R_{xy}(i\nu_m) = -\frac{ie^2v_F^2}{2\pi\ell_B^2\beta\hbar}(2\sum_{\substack{\mu,\nu\\=\pm}}\chi^{\mu\nu,+\nu}_{1,0} + \sum_{\ell\geq 1}\sum_{\substack{\mu,\rho\\=\pm}}\sum_{\nu=\pm}\chi^{\mu\nu,\rho\nu}_{\ell+1,\ell}), \tag{9}$$

where $\chi^{\mu\nu,\rho\sigma}_{k,\ell}$ is defined as

$$\chi^{\mu\nu,\rho\sigma}_{k,\ell}(i\nu_m) = \sum_{n=-\infty}^{n=\infty}[\frac{1}{(i\tilde{\omega}_n - \tilde{E}^{\mu\nu}_k)(i\tilde{\omega} + i\nu_m - \tilde{E}^{\rho\nu}_\ell)} - (i\nu_m \to -i\nu_m)]. \tag{10}$$

In the DC and clean limit, we let $\Omega + i0 \to 0$ and set $\Gamma = 0$. Then, after evaluating the Matsubara sums[15], we find that

$$\frac{1}{\beta\hbar}\chi^{\mu\nu,\rho\sigma}_{k,\ell}|_{i\nu_m=\Omega+i0\to 0} \approx \frac{-2(\Omega+i0)[f(E^{\mu\nu}_k) - f(E^{\rho\sigma}_\ell)]}{(\tilde{E}^{\mu\nu}_k - \tilde{E}^{\rho\sigma}_\ell)^2}, \tag{11}$$

where $f(E)$ is the Fermi-Dirac distribution. Furthermore, we define $\tilde{f}(E) = f(E) - 1/2$. Then, using Eqs. (7), (9) and (11) and considering the variation of direction of conductivity with the signs of magnet field and carrier charge, we can derive that

$$\sigma_{xy} = -\frac{4e^2}{h}\mathrm{sgn}(eB)\left[\sum_{\nu=\pm}\tilde{f}(E^{+\nu}_0) + \sum_{\ell\geq 1}^{\infty}\sum_{\substack{\mu,\nu\\=\pm}}\tilde{f}(E^{\mu\nu}_\ell)\right] \tag{12}$$

At zero temperature, $f(E) = 1$ and $f(E) = 0$ for the occupied and unoccupied LLs, respectively. The LLs located at $E \leq \bar{\mu}$ are ocuppied and the others are empty. That is to say, $\tilde{f}(E) = 1/2$ for $E \leq \bar{\mu}$, while $\tilde{f}(E) = -1/2$ for $E > \bar{\mu}$. Therefore, we only need to calculate the number of LLs between $-\bar{\mu}$ and $\bar{\mu}$ to determine the magnitude of the Hall conductivity. Moreover, for $-|\bar{\mu}| < E < |\bar{\mu}|$, the number of the up-shifted LLs ($\nu = -$) is equal to that of the down-shifted LLs ($\nu = +$). Hence, we find that the zero-temperature Hall conductivity is given by

$$\sigma_{xy} = -\frac{4e^2}{h}\mathrm{sgn}(\bar{\mu})\mathrm{sgn}(eB)\,[\theta(|\bar{\mu}|+t)\theta(|\bar{\mu}|-t) + \sum_{\ell\geq 1}^{\infty}\sum_{\mu=\pm}\theta(|\bar{\mu}| - E^{\mu-}_\ell)\theta(|\bar{\mu}| + E^{\mu-}_\ell)\,]. \tag{13}$$

Eq. (13) indicates that the Hall conductivity would simply change its sign as $\bar{\mu} \to -\bar{\mu}$ and that the Hall conductivity is equal to $4e^2/h$ times the number of up-shifted LLs between $-|\bar{\mu}|$ and $|\bar{\mu}|$. Eq. (13) can also be written in the form

$$\begin{aligned}\sigma_{xy} = &-\frac{4e^2}{h}\mathrm{sgn}(\bar{\mu})\mathrm{sgn}(eB)\times\\ &\left\{\theta(|\bar{\mu}| - t - \sqrt{2\hbar v_F^2|eB|/c})\left[\frac{c(|\bar{\mu}|-t)^2}{2\hbar v_F^2|eB|}\right]\right.\\ &+\theta(\sqrt{2\hbar v_F^2|eB|/c} - t + |\bar{\mu}|)\left[\frac{c(|\bar{\mu}|-t)^2}{2\hbar v_F^2|eB|}\right]\\ &+\left[\frac{c(|\bar{\mu}|+t)^2}{2\hbar v_F^2|eB|}\right] - \left[\frac{c(|\bar{\mu}|-t)^2}{2\hbar v_F^2|eB|}\right]\\ &\left.+\,\theta(|\bar{\mu}|+t)\theta(|\bar{\mu}|-t)\right\}.\end{aligned} \tag{14}$$

Here $[x]$ means the integer part of x. The last term is the contribution of level anomalies ($N = 0$)[4].

We also calculate the longitudinal conductivity (σ_{xx}) via the Kubo formula. The longitudinal conductivity have to be evaluated under the effect of disorder scattering ($\Gamma \neq 0$). Using Cauchy's integral theorem as in Refs. [16, 17], we can obtain

$$\sigma_{xx} = \frac{e^2}{\pi h}\omega_c^2\left\{\int_{-\infty}^{\infty}dE\left(-\frac{\partial f}{\partial E}\right)\times \left[\sum_{\substack{\mu,\rho\\=\pm}}\sum_{\nu=\pm}\sum_{\ell\geq 1}^{\infty}\mathrm{Im}\tilde{g}^{\mu\nu}_{\ell+1}(E)\mathrm{Im}\tilde{g}^{\rho\nu}_\ell(E) + 2\sum_{\substack{\mu,\nu\\=\pm}}\mathrm{Im}\tilde{g}^{\mu\nu}_1(E)\mathrm{Im}\tilde{g}^{+\nu}_0(E)\right]\right\}, \tag{15}$$

where $\tilde{g}^\rho_\ell = 1/(E/\hbar - \tilde{E}^{\rho\nu}_\ell + i\Gamma/\hbar)$. Applying the techniques of partial-fraction decomposition similar to that used in Ref. [18] and after some cumbersome algebra, we finally find that the zero-temperature longitudinal conductivity can be written in terms of the digamma func-

tion (φ_0)[19],

$$\sigma_{xx} = \frac{4e^2}{\pi h}\sum_{\nu=\pm}\Bigg\{ i\left[\varphi_0\left(-\frac{(\bar{\mu}+\nu t)^2-\Gamma^2}{\hbar^2\omega_c^2}+1-i\frac{2\Gamma(\bar{\mu}+\nu t)}{\hbar^2\omega_c^2}\right)\right.$$
$$\left.-\,\varphi_0\left(-\frac{(\bar{\mu}+\nu t)^2-\Gamma^2}{\hbar^2\omega_c^2}+1+i\frac{2\Gamma(\bar{\mu}+\nu t)}{\hbar^2\omega_c^2}\right)\right]$$
$$\times\frac{\left[2(\bar{\mu}+\nu t)^3\Gamma+2(\bar{\mu}+\nu t)\Gamma^3\right]}{p}$$
$$+\frac{\left[\hbar^6\omega_c^6+\hbar^4\omega_c^4(\bar{\mu}+\nu t)^2-12\hbar^2\omega_c^2(\bar{\mu}+\nu t)^4+8(\bar{\mu}+\nu t)^6\right]\Gamma^2}{q}$$
$$+\frac{\left[\hbar^4\omega_c^4+4\hbar^2\omega_c^2(\bar{\mu}+\nu t)^2+16(\bar{\mu}+\nu t)^4\right]\Gamma^4}{q}$$
$$+\frac{8(\bar{\mu}+\nu t)^2\Gamma^6}{q}$$
$$+\frac{\left[\hbar^2\omega_c^2(\bar{\mu}+\nu t)^2+\hbar^4\omega_c^4\right]\Gamma^2+\hbar^2\omega_c^2\Gamma^4}{\left[(\bar{\mu}+\hbar\omega_c+\nu t)^2+\Gamma^2\right]\left[(\bar{\mu}-\hbar\omega_c+\nu t)^2+\Gamma^2\right]}$$
$$\times\frac{1}{(\bar{\mu}+\nu t)^2+\Gamma^2}\Bigg\}. \qquad (16)$$

Here,

$$p=\hbar^4\omega_c^4+16\Gamma^2(\bar{\mu}+\nu t)^2,$$
$$q=\left\{[(\bar{\mu}+\nu t)^2-\hbar^2\omega_c^2-\Gamma^2]^2+4\Gamma^2(\bar{\mu}+\nu t)^2\right\}\times p. \qquad (17)$$

Unlike Ref. 20, we do not adopt low-magnetic field approximation here and therefore Eq. (16) is general and suitable for all values of the applied magnetic field. However, when we adopt the low-disorder and high-magnetic-field limit, we first consider Γ as being small and keep the terms in the order of Γ^2. Then, we let $(\bar{\mu}+\nu t)/(\hbar^4\omega_c^4)\to 0$, Eq. (16) could be simplified as

$$\sigma_{xx}\approx\frac{4e^2}{\pi h}\left[\frac{(\bar{\mu}^2+t^2)\Gamma^2}{(\bar{\mu}^2-t^2)^2}+2\frac{\Gamma^2}{\hbar^2\omega_c^2}+5\frac{\bar{\mu}^2+t^2}{\hbar^2\omega_c^2}\frac{\Gamma^2}{\hbar^2\omega_c^2}\right]. \qquad (18)$$

The first term is independent of B. The second and third terms are proportional to $1/B$ and $1/B^2$, respectively.

III. DEPENDENCE OF CONDUCTIVITY ON MAGNETIC FIELD AND CHEMICAL POTENTIAL

Since both the magnetic field and chemical potential could be tuned experimentally, we display the calculated conductivity as a function of $1/B$ and $\bar{\mu}$ in this Sec. Here we use the interlayer hopping energy $t = 0.2$ eV for the AA-stacking and $t = 0.4$ eV for the AB-stacking as determined by the *ab initio* DFT calculations within the local density approximation (LDA)[21]. Moreover, because the quantized values of the Hall conductivity is independent of the presence of disorder scattering[22], we show only the Hall conductivity in the clean limit (i.e., $\Gamma = 0$) and analyze the Hall plateaus qualitatively.

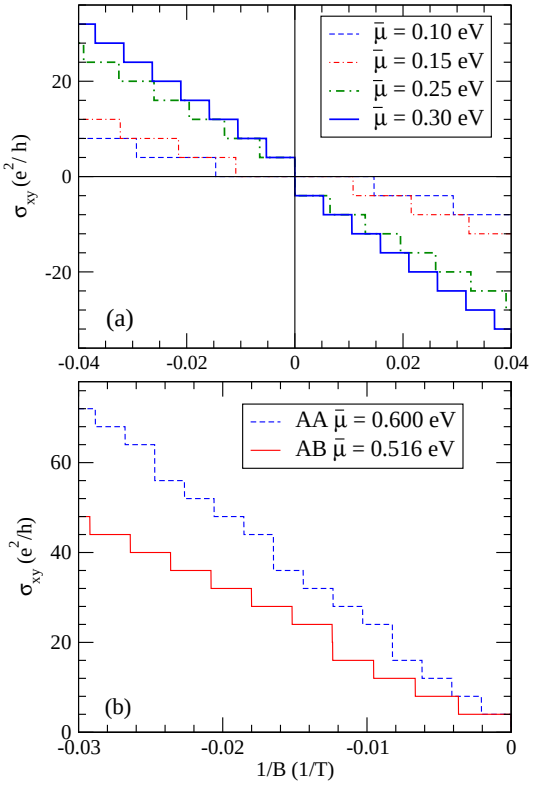

FIG. 2: (color online) (a) The quantized Hall conductivity σ_{xy} of the AA-stacked bilayer graphene as a function of $1/B$ for several values of chemical potential $\bar{\mu}$. (b) The quantized Hall conductivity σ_{xy} of both AA-stacked and AB-stacked bilayer graphenes as a function of $1/B$. The interlayer hopping energy t used is 0.2 eV for the AA-stacking and 0.4 eV for the AB-stacking, and $v_F = 1.0\times10^6$ m/s. The Hall conductivity σ_{xy} for the AB-stacking was obtained by using Eq. 15 from Ref. 10.

A. Conductivities vs inverse of magnetic field

In Fig. 2, the Hall conductivity is plotted as a function of $1/B$ and we should discuss the effect of chemical potential on the σ_{xy} vs. $1/B$ curve. From Fig. 2(a), we see that $\sigma_{xy} = \pm\frac{4e^2}{h}n$, with $n = 0, 1, 2, \cdots$, for $|\bar{\mu}| < t$, and $n = 1, 2, 3, \cdots$, for $|\bar{\mu}| > t$, excluding $|\bar{\mu}| = [(\sqrt{n_2}+\sqrt{n_1})/(\sqrt{n_2}-\sqrt{n_1})]t$, where $n_1 = 1, 2, 3, \cdots$ and $n_2 = 2, 3, 4, \cdots$. It is clear from either Eq. (13) or Eq. (14) that $\sigma_{xy}(-\bar{\mu}) = -\sigma_{xy}(\bar{\mu})$, and hence we did not show any curves for $\bar{\mu} < 0$ in Fig. 2(a). Interestingly, in constrast to the MLG and AB-stacked BLG, the AA-stacked BLG displays the pronounced $\bar{\nu} = 0$ plateau for $|\bar{\mu}| < t$, where the filling factor $\bar{\nu} = \sigma_{xy}h/e^2$. The MLG and AB-stacked BLG lack the $\bar{\nu} = 0$ plateau because their level anomalies are located at $E = 0$. The level anomaly of the MLG is the zeroth Landau level while those of the AB-stacked BLG are the zeroth and first Landau levels. The occurrence of level anomalies is a remarkable manifestation of the unique property of chiral quasiparticles[8, 23]. In the AA-stacked BLG, similarly, level anomalies also

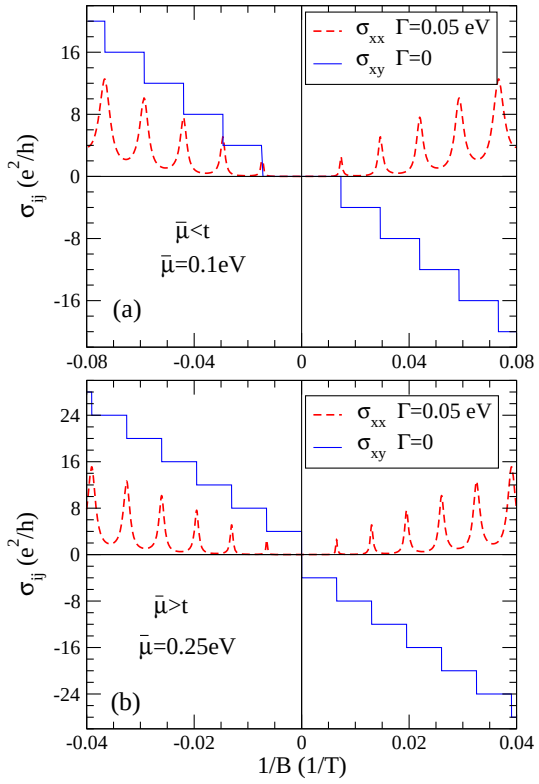

FIG. 3: (color online) The longitudinal (σ_{xx}) and transverse (σ_{xy}) conductivities of the AA-stacked bilayer graphene as a fuction of $1/B$, (a) for $|\bar{\mu}| < t$, and (b) for $|\bar{\mu}| > t$. The rest parameters are the same as in Fig. 2.

exist in the LL spectrum. However, for the AA-stacked BLG, the level anomalies are shifted up and down by t, respectively. Thus, these level anomalies are unique in the sense that they are always located at the Dirac points regardless of the magnitude of B, in contrast with the other Landau levels[4, 8, 10]. It is worth mentioning that the Dirac points often exhibit interesting electronic properties, such as electron-hole puddle formation[24, 25], and Andreev reflection type transitions.[26] Untill now, some transport properties at these Dirac points remain to be understood[27]. The level anomaly is one of the interesting properties of the Dirac points and recently the nature of its electronic states (being metallic or insulating) in the high magnetic field-low temperature regime is hotly debated[28].

Displayed in Fig. 2(b) are the Hall plateaus of the AA-stacked BLG for $|\bar{\mu}| = [(\sqrt{n_2}+\sqrt{n_1})/(\sqrt{n_2}-\sqrt{n_1})]t$. We find that in addition to the $\bar{\nu} = 0$ plateau, other differences between the AA-stacked and AB-stacked BLGs exist. In particular, when $|\bar{\mu}| = [(\sqrt{n_2}+\sqrt{n_1})/(\sqrt{n_2}-\sqrt{n_1})]t$, some $8e^2/h$-steps appear at $1/B \neq 0$. In other words, in comparison with the other cases of $|\bar{\mu}| > t$ ($|\bar{\mu}| \neq [(\sqrt{n_1}+\sqrt{n_2})/(\sqrt{n_2}-\sqrt{n_1})]$), some plateaus would be missing for $|\bar{\mu}| = [(\sqrt{n_2}+\sqrt{n_1})/(\sqrt{n_2}-\sqrt{n_1})]t$. Furthermore, these $8e^2/h$-steps appear periodically. Taking $\bar{\mu} = 3t$ (i.e. $n_2 = 4, n_1 = 1$), for example, between any two $8e^2/h$-steps, the curve passes through three $4e^2/h$-steps and four plateaus. Only the Hall plateaus $\sigma_{xy} = \frac{4e^2}{h}n$, $n = \pm1, \pm2, \pm3, \pm4, \pm6, \pm7, \pm8, \pm9, \pm11, \pm12, \cdots$, appear. In other words, the Hall plateaus $n = \pm5, \pm10, \pm15, \cdots$ are absent here. When $|\bar{\mu}| > t$, the quantum Hall effect of the AB-stacked BLG must be studied based on a four-band Hamiltonian[10]. Based on the four-band model[10], for $|\bar{\mu}| > t$, the AB-stacked BLG can also exhibit a $8e^2/h$-step, as shown in Fig. 2(b). Although the $8e^2/h$-step is not specific to the AA-stacked BLG, the periodic appearance of the $8e^2/h$-steps has never been seen in the AB-stacked BLG and hence is a unique characteristic of the AA-stacked BLG.

The longitudinal and transverse conductivities as a fuction of $1/B$ are plotted together in Fig. 3. It is seen from Fig. 3 that the longitudinal conductivity goes to a local minima at the position of the Hall plateaus and reaches a local maxima as the steps appear except the step at $1/B = 0$. The unique $\bar{\nu} = 0$ Hall plateau of the AA-stacked bilayer graphene for $|\bar{\mu}| < t$ is especially interesting. From Fig. 3(a), we find that σ_{xx} falls to zero as the $\bar{\nu} = 0$ Hall plateau emerges. As stated previously, for $|\bar{\mu}| > t$, the AA-stacked BLG lacks the $\bar{\nu} = 0$ Hall plateau. The first Hall plateau occurs at $\bar{\nu} = 4$ or $\bar{\nu} = -4$. This encourages us to investigate the difference between the longitudinal conductivities at the $\bar{\nu} = 0$ Hall plateau for $|\bar{\mu}| < t$ and at the $\bar{\nu} = \pm4$ Hall plateaus for $|\bar{\mu}| > t$. Fig. 3(b) shows that for $|\bar{\mu}| > t$, the σ_{xx} goes to zero as the first Hall plateau occurs. This implies that at the high magnetic field, the external electric field cannot drive any current for $|\bar{\mu}| < t$ while the current is perpendicular to the external electric field for $|\bar{\mu}| > t$. Here $\bar{\mu}$ and t are in the order of 0.1 eV while the order of magnitude of Γ [$\mathcal{O}(\Gamma)$] is 0.01 eV. $\bar{\mu} + \nu t$ are about one order of magnitude higher than Γ ($\bar{\mu} + \nu t \sim 10\Gamma$). Therefore, the condition of low disorder is satisfied. If $\hbar^4\omega_c^4 \gg (\bar{\mu} + \nu t)$, Eq. (18) can be applied here. This needs $\hbar\omega_c$ to be larger than 1.78 $(\bar{\mu} + \nu t)$ and B is estimated to be at least a few times larger than 10 T. In the low-disorder and high-magnetic-field regime, we roughly estimate from Eq. (18)

$$\sigma_{xx} \sim \frac{4e^2}{h}\left[\frac{2}{\pi}\frac{(\bar{\mu}^2+t^2)\Gamma^2}{(\bar{\mu}^2-t^2)^2} + \mathcal{O}(0.001)\right]. \qquad (19)$$

When $\mathcal{O}(|\bar{\mu}| - t) \geq 1\Gamma$, $\sigma_{xx} \sim 0.1(4e^2/h) \to 0$.

Interestingly, the results shown in Fig. 2 could be explained in terms of Fig. 4. Let us account for Fig. 2(a) first. It is clear from Fig. 4 that for $|\bar{\mu}| < t$, level anomalies are outside the range of $-|\bar{\mu}| \sim |\bar{\mu}|$. Conversely, for $|\bar{\mu}| > t$, level anomalies are inside the range of $-|\bar{\mu}| \sim |\bar{\mu}|$. In the high magnetic field regime, for $|\bar{\mu}| < t$, no Landau level exists between $-|\bar{\mu}|$ and $|\bar{\mu}|$ and hence the AA-stacked BLG displays the conventional insulating behaviour (a $\bar{\nu} = 0$ Hall plateau) even though it possesses chirality. Such behaviour of the AA-stacked BLG is in stark contrast to the MLG and AB-stacked BLG. However, for $|\bar{\mu}| > t$, level anomalies are located between $-|\bar{\mu}|$

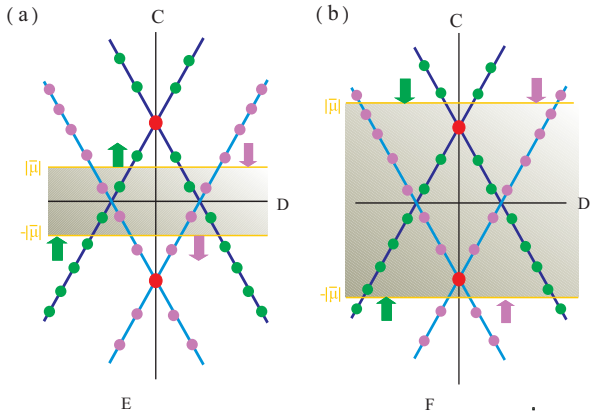

FIG. 4: (color) The Landau level spectrum of the AA-stacked bilayer graphene (a) with $|\bar{\mu}| < t$ and (b) with $|\bar{\mu}| > t$, respectively. Here circles mark the positions of Landau levels. Red, green, and purple circles represent the locations of level anomalies as well as other up-shifted and down-shifted Landau levels, respectively. Mazarine and blue lines denote the up-shifted and down-shifted energy bands, respectively. Shaded is the region between $-\bar{\mu}$ and $|\bar{\mu}|$.

and $|\bar{\mu}|$ even in the high magnetic field regime and hence a $\bar{\nu} = 0$ plateau cannot emerge.

The Hall plateaus displayed in Fig. 2(b) can be explained as follows. A up-shifted LL of $E_k^{-\mu,-}$ and a down-shifted LL of $E_k^{\mu,+}$ are partners because $E_k^{\mu,+} = -E_k^{-\mu,-}$. As the up-shifted LL of $E_k^{-\mu,-}$ goes through the $|\bar{\mu}|$-level, the down-shifted LL of $E_k^{\mu,+}$ passes through the $-|\bar{\mu}|$-level. They always enter the region between $|\bar{\mu}|$ and $-|\bar{\mu}|$ (i.e. the shaded region) together and hence each contribute $4e^2/h$ to the Hall conductivity. Therefore, the Hall conductivity is equal to $4e^2/h$ times the number of either up-shifted or down-shifted LLs between $-|\bar{\mu}|$ and $|\bar{\mu}|$. Therefore, in order to form a $8e^2/h$-step, either two up-shifted or down-shifted LLs must enter or leave the shaded region together. Hence we only need to focus on either up-shifted or down-shifted Dirac cones and discuss the movement of the LLs located in this cone to explain the origin of $8e^2/h$-steps. Let us consider the up-shifted Dirac cone. As the magnetic field decreases gradually, the up-shifted LLs would go close to its level anomaly, $E = t$. Therefore, we can infer that for $|\bar{\mu}| < t$, the LLs above the $|\bar{\mu}|$-level (called the upper LLs) go far away from the $|\bar{\mu}|$-level, while the LLs below the $-|\bar{\mu}|$-level (called the lower LLs) move toward the $-|\bar{\mu}|$-level, as shown in Fig. 4(a). The lower LLs would enter the shaded region one by one but the upper LLs can never get into the shaded region. However, for $|\bar{\mu}| > t$, both the upper and lower LLs can go close to the shaded region [see Fig. 4(b)], i.e., two up-shifted LLs may enter the shaded region together. Therefore, the $8e^2/h$-steps can only appear when $|\bar{\mu}| > t$.

For brevity, we use indices (k, μ, ν) to denote the Landau level of $E_k^{\mu,\nu}$ below. Let us label the two LLs which enter the shaded region together as the $(k_1, -, -)$ and $(k_2, +, -)$ LLs. Then, $k_1/k_2 = (|\bar{\mu}| - t)^2/(|\bar{\mu}| + t)^2$. (n_1, n_2) satisfies this condition and n_1/n_2 is an irreducible fraction. Then, $(k_1, k_2) = (pn_1, pn_2)$, where $p = 1, 2, 3\cdots$, is a set of solutions of $k_1/k_2 = (|\bar{\mu}|-t)^2/(|\bar{\mu}|+t)^2$. Between the entries of $[(p-1)n_1, (p-1)n_2]$ and $[pn_1, pn_2]$ LLs, (n_1+n_2-2) LLs get into the shaded region sequentially as $1/B$ decreases. Hence, (n_1+n_2-2) $4e^2/h$-steps occur between any two $8e^2/h$-steps. The Hall conductivity is quantized as $\sigma_{xy} = \pm\frac{4e^2}{h}n$ with the exception of $\pm\frac{4e^2}{h}(n_1+n_2)n$, where $n = 1, 2, 3, \cdots$, as shown in Fig. 2(b). Unlike the AB-stacked BLG and the other cases of $|\bar{\mu}| > t$ of the AA-stacked BLG, the Hall conductivity for $|\bar{\mu}| = [(\sqrt{n_2}+\sqrt{n_1})/(\sqrt{n_2}-\sqrt{n_1})]t$ lacks the $\bar{\nu} = \pm 4(n_1+n_2)n$ plateaus. Furthermore, it is clear from Fig. 2(b) that when $|\bar{\mu}| > t$, the AB-stacked BLG can also exhibit a $8e^2/h$-step but the appearance of the $8e^2/h$-steps is not periodical. The main findings here are summarized in Table I.

TABLE I: The characteristics of integer quantum Hall effect in monolayer (ML), AB-stacked bilayer (AB) and AA-stacked bilayer (AA) graphenes as well as conventional two-dimensional semiconductor structures (2D).

	ML	AB	AA	2D
plateau steps ($\frac{e^2}{h}$)	4	4, 8[a]	4, 8[b]	2
$\bar{\nu} = 0$ plateau	no	no	yes[c]	yes

[a] The $8\frac{e^2}{h}$ plateau step only occurs (aperiodically) in the four band model (Ref. [10]).
[b] The $8\frac{e^2}{h}$ plateau step appears periodically for $|\bar{\mu}| > t$ only.
[c] The $\bar{\nu} = 0$ plateau occurs only if $|\bar{\mu}| < t$.

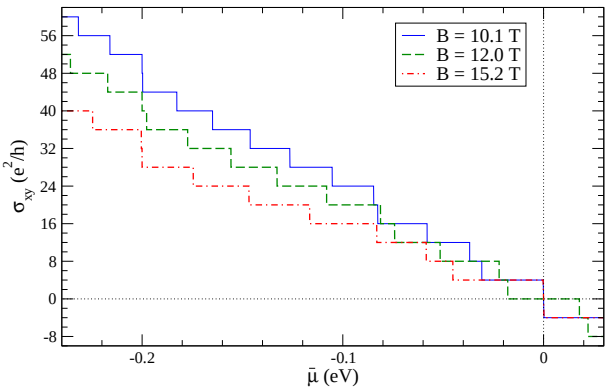

FIG. 5: (color online) The quantized Hall conductivity σ_{xy} of the AA-stacked bilayer graphene as a function of chemical potential $\bar{\mu}$ for several values of magnetic field B. The rest parameters are the same as in Fig. 2.

B. Hall conductivity vs chemical potential

Fig. 5 is a plot of σ_{xy} versus $\bar{\mu}$, showing how the Hall plateaus are influenced by the magnetic field. It is clear from Fig. 4 that unlike the MLG and AB-stacked BLG, a $\bar{\nu} = 0$ plateau centered at $\bar{\mu} = 0$ appears for $B = 12$

T in the AA-stacked BLG. However, when the condition of $\sqrt{2N}\hbar v_F/\ell_B = t$ is reached by tuning the magnetic field, the $(N,+,-)$ and $(N,-,+)$ LLs would be located at $E = 0$. As a result, the $\bar{\nu} = 0$ plateau disappears and a $8e^2/h$-step at $\bar{\mu} = 0$ forms, like the AB-stacked BLG. In other words, the absence of the $\bar{\nu} = 0$ plateau needs the magnetic field $B = \pi t^2/Nehv_F^2$, where $N = 1, 2\cdot\cdot$. In Fig. 5, $B = 10.1$ T and $B = 15.2$ T satisfy this condition with $N = 3$ and $N = 2$, respectively. Thus, these curves lack the $\bar{\nu} = 0$ plateau.

In addition, we note that a $8e^2/h$-step occurs at $\bar{\nu} = t$ for $B = 10.1$ T and $B = 15.2$ T. For $B = 12$ T, all the LLs are nondegenerate and hence all the steps are of the height of $4e^2/h$. However, if the $(N,-,+)$ and $(o,+,-)$ LLs are degenerate at $E = t$, a $8e^2/h$-step appears at $\bar{\mu} = t$. This level degeneracy happens as the magnetic field $B = 4\pi t^2/Nehv_F^2$, where $N = 1, 2, 3, \cdots$. $B = 10.1$ T and $B = 15.2$ T fit the condition with $N = 3$ and $N = 2$, respectively, and thus a $8e^2/h$-step appears at $\bar{\mu} = t$. We also find that the disappearance of a zero-Hall conductivity plateau is always accompanied by the occurence of a $8e^2/h$-step at $\bar{\mu} = t$, because if $B = \pi t^2/Nehv_F^2$, B would satisfy $B = 4\pi t^2/N'ehv_F^2$ with $N' = 4N$. Interestingly, here we find that the structure of the Hall plateaus of the AA-stacked BLG would be significantly affected by the applied magnetic field, which is quite different from the MLG and the AB-stacked BLG.

IV. SUMMARY

In conclusion, we have calculated both the quantized Hall conductivity and longitudinal conductivity of the AA-stacked bilayer graphene within linear response theory by using Kubo formula. We find that the dependence of the Hall plateau of the AA-stacked BLG on the magnetic field is distinctly different from both the MLG and AB-stacked BLG as well as the conventional quantun Hall materials. In particular, the AA-stacked bilayer graphene could possess the unique $\bar{\nu} = 0$ plateau, in contrast to other graphene materials such as monolayer and AB-stacked bilayer graphene. The shift of level anomalies due to interlayer hopping energy is attributed to be the origin of the $\bar{\nu} = 0$ plateau. Nonetheless, the $\bar{\nu} = 0$ plateau across $\bar{\mu} = 0$ would disappear if magnetic field $B = \pi t^2/Nehv_F^2$. In addition, we find that the disappearance of a zero-Hall conductivity plateau is always accompanied by the occurence of a $8e^2/h$-step at $\bar{\mu} = t$. Furthermore, when $|\bar{\mu}| = [(\sqrt{n_1}+\sqrt{n_2})/(\sqrt{n_2}-\sqrt{n_1})]t$, the AA-stacked BLG lacks the $\bar{\nu} = \pm 4(n_1+n_2)n$ plateaus, which exist in the AB-stacked BLG. We also find that when $\Gamma \to 0$ and $\hbar^4\omega_c^4 \gg (\bar{\mu}+\nu t)^4$, $\sigma_{xx} \to 0$ if the Fermi level is not a few Γs above and below a Dirac point. This implies that at the high magnetic field, the external electric field cannot drive any current for $\bar{\mu} < t$ while the current would be perpendicular to the external electric field for $\bar{\mu} > t$. We hope that our predicted interesting characteristics of quantum Hall effect in the AA-stacked BLG, which are not seen in both the MLG and BLG as well as the conventional quantum Hall materials, would stimulate experimental effort on fabricating the AA-stacked BLG and also on measurement of its transport property in the near future.

ACKNOWLEGEMENTS

The authors thank Hung-Yu Yeh, Tsung-Wei Chen and Ming-Che Chang for valuable discussions. The authors also acknowledge financial supports from National Science Council and NCTS of Taiwan.

[1] A. H. Castro Neto, N. M. R. Peres, K. S. Novoselov, and A. K. Geim, Rev. Mod. Phys. **81**, 109 (2009).
[2] P. R. Wallace, Phys. Rev. **71**, 622 (1947)
[3] M. I. Katsnelson, K. S. Novoselov, And A. K. Geim, Nat. Phys. **2**, 620 (2006).
[4] V.P. Gusynin, and S.G. Sharapov, Phys. Rev. Lett. **95**, 146801 (2005).
[5] K. S. Novoselov, A. K. Geim, S. V. Morozov, D. Jiang, M. I. Katsnelson, I. V. Grigorieva, S. V. Dubonos and A. A. Firsov, Nature (London) **438**, 197 (2005).
[6] Y. Zhang, Y. W. Tan, H. L. Stormer, and P. Kim, Nature (London) **438**, 201 (2005).
[7] K.S. Novoselov,Z. Jiang, Y. Zhang, S. V. Morozov, H. L. Stormer, U. Zeitler, J. C. Maan, G. S. Boebinger, P. Kim, and A.K. Geim, Science **315**, 1379 (2007).
[8] E. McCann and V. I. Fal'ko, Phys. Rev. Lett. **96**, 086805 (2006).
[9] K. S. Novoselov1, E. McCann, S. V. Morozov, V. I. Fal'ko, M. I. Katsnelson, U. Zeitler, D. Jiang, F. Schedin and A. K. Geim, Nat. Phys. **2**, 177 (2006).
[10] M. Nakamura, L. Hirasawa, and K.-I. Imura, Phys. Rev. B **78**, 033403 (2008).
[11] M. Aoki and H. Amawashi, Solid State Commun. **142**, 123(2007).
[12] P. L. de Andres, R. RamÍrez, and J. A. Vergés, Phys. Rev. B **77**, 045403 (2008).
[13] P. Lauffer, K. V. Emtsev, R. Graupner, Th. Seyller, and L. Ley, Phys. Rev. B **77**, 155426 (2006).
[14] Z. Liu, K. Suenagam, H. Suzuura, P. J. F. Harris, and S. Iijima, Phys. Rev. Lett. **102**, 015501 (2009).
[15] H. Bruus, and K. Flensberg, Many-Body Quantum Theory in Condensed Matter Physics (Oxford, New York, 2007), Chaps. 6 and 11.
[16] G. D. Mahan, Many-Particle Physics (Plenum Press, New York, 2000), Chap. 4.
[17] M. Iwasaki, H. Ohnishi and T. Fukutome, J. Phys. G: Nucl. Part. Phys. **35**, 035003 (2008).
[18] A. Endo, N. Hatano2, H. Nakamura, and R. Shirasaki, J. Phys. : Condens. Matter **21**, 345803 (2009).
[19] N. N. Lebedev, Special Functions and Their Applications

(Dover, New York, 1972), Chap. 1.
[20] V. P. Gusynin, and S. G. Sharapov, Phy. Rev. B **71**, 125124 (1972).
[21] H. Y. Yeh (private communication).
[22] M. Janβen, O. Veihweger, U. Fastenrath, and J. Hajdu, Introduction to the Theory of the Integer Quantum Hall Effect (VCH, Weinheim, 1994).
[23] D.Yoshioka, The Quantum Hall effect (Spring-Verlag, Berlin Heidelberg, 2002), Chap. 7.
[24] E. H. Hwang, S. Adam, and S. Das Saima, Phys. Rev. Lett. **98**, 186806 (2007).
[25] J. Martin, N. Akerman, G. Ulbricht, T. Lohmann, J. H. Smet, K. Von Klitzing, and A. Yacoby, Nat. Phys. **4**, 144 (2008).
[26] Y. F. Hsu, and G. Y. Guo, Phys. Rev. B **81**, 045412 (2010).
[27] A. K. Geim, Science **324**, 1530 (2004).
[28] L. Zhang, Y. Zhang, M. Khodas, T. Valla, and I. A. Zaliznyak, arXiv:1003.2738 (2010).